ARTICLES

Molecular Dynamics Study of Tribological Behavior of Confined Branched and Linear Perfluoropolyethers

Asako Koike

Hitachi Research Laboratory, Hitachi, Ltd., 7-1-1 Omika, Hitachi, Ibaraki 319-1292, Japan

Received: November 10, 1998; In Final Form: March 31, 1999

Molecular dynamics simulations have been performed to study the rheological behavior of confined branched (Krytox type and Fomblin Y type) and linear (Demnum type and Fomblin Z type) perfluoropolyethers. Shear thinning of the viscosity is observed in all cases, and the shear thinning rate is in reasonable agreement with experimental results of Demnum and Krytox types. The viscosity of the branched Krytox type is slightly lower than that of the linear Demnum type when confined, although their bulk viscosity values are the same. Further, higher molecular ordering is observed in the Demnum type than in the Krytox type. However, no viscosity difference is observed between branched Fomblin Y and linear Fomblin Z types, which have many ether linkages. No molecular order difference is observed between them either. Accordingly, the side chain effect is expected to decrease because of the molecular flexibility caused by their many ether linkages. The nonbonded interaction energy between an atom and atoms of other molecules is also investigated as a function of the sliding distance using different slider velocities. It is found that short periodic energy changes decrease and long periodic energy changes increase with increasing slider velocity. This is expected to be one of the causes of the decrease in the energy required for the molecules to pass each other within a certain distance and one of the causes for shear thinning.

1. Introduction

The study of boundary lubrication of thin organic films is crucial in various fields from basic science to industrial applications such as micromachines, magnetic storage devices, and automobile engines. For example, in the case of magnetic storage devices, thin film lubricants are coated on the disk surfaces to prevent the magnetic layers from being crushed because of the friction between the head and the disk surfaces.[1−3] With the rapid raise of recording densities in recent years, the flying height as a distance between the disk surface and the head decreases in order to minimize the loss of the magnetic signal and the sliding condition becomes more severe for lubricants. Further, from the viewpoint of static friction at the beginning of the rotation of the disk, the film thickness must be a minimum and the actual lubricant layers must be thinner than 2 nm.[4] Accordingly, thin film, low friction, no-wear, and durable lubricants must be developed and they must be studied under shear.

Recent results obtained from a surface force apparatus (SFA)[5−11] and computer simulations[12−21] have revealed that the static and dynamic properties of confined films are strikingly different from their bulk properties. For example, oscillatory solvation force profiles have been observed as a function of the film thickness for less than several molecular thicknesses[5] and the oscillation strength was seen to be weakened by the effects of branching.[6] This behavior was reproduced by computer simulations.[12,13] The viscosity of a confined thin film was found to be several orders higher than the bulk values.[7] The effect of branching on the shear viscosity was also investigated.[8,14−21] Regarding shear behavior in hydrocarbons, computer simulations showed that linear molecules line up more easily than branched molecules[14,15,19] and the ratio of the power law decrease of viscosity with shear rate depends on the side chain and its position.[16] When the number of side chains is one and the side chain is short, branched molecules have almost the same viscosity as linear molecules.[16] On the other hand, when the side chain is long or there are multiple side chains, the viscosity of the branched molecules is higher than that of linear molecules.[15,19] However, there are no distinct differences in viscosities and shear behavior of a confined thin film at high shear rate obtained experimentally. By contrast, for perfluoropolyethers, remarkable differences between linear and branched molecules in the confined state have been observed in experiments.[9−11] Although the shear stress decreases with increasing shear rate in linear molecules (Fomblin Z), it increases with increasing shear rate in branched molecules (Fomblin Y).[22] Further, the viscosity of linear molecules is significantly higher than that of branched molecules, while the bulk viscosity of the former is an order lower than the latter's and both viscosities are several orders of magnitude higher than the bulk values.[9] The linear response of the periodic shear shows that although the branched molecules (Krytox)[23] are fluidlike at the measurable frequencies of the SFA, the linear molecules (Demnum)[24] are easily solidified.[11] The transition from linear response to nonlinear response is discontinuous in linear molecules and continuous in branched molecules. Further, the effective viscosity of the linear molecules as a linear response is significantly higher than that of branched molecules, while both viscosities

10.1021/jp984379b CCC: $18.00
Published on Web 05/18/1999

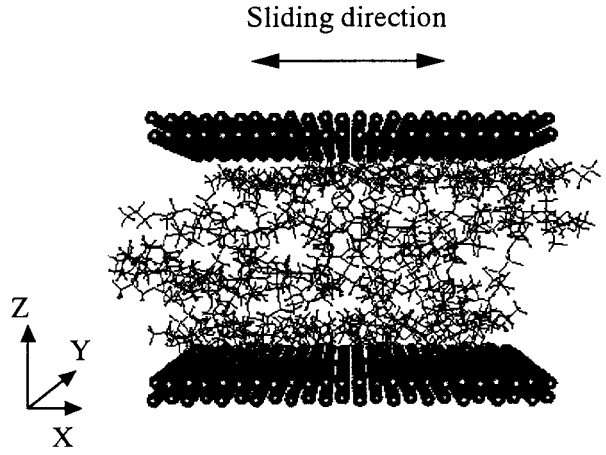

Figure 1. Initial configuration of confined Krytox long type molecules.

are almost the same under the bulk conditions.[11] Both studies (Fomblin Y and Fomblin Z,[9] Demnum and Krytox[11]) show that the branched molecules are less restricted and have low viscosities. On the other hand, Pooley and Tabor[25] showed that branched molecules of perfluoroalkanes have larger shear stress than linear molecules (poly(tetrafluoroethylene)) and they concluded that the side chain prevents the molecules from lining up and makes the frictional coefficient become larger. In their experiment, the film was not liquid but semicrystallite.

These perfluoropolyethers, Demnum, Krytox, Fomblin Z, and Fomblin Y, are widely used as lubricants in magnetic recording disks. However, the measured shear rate (10 to 10^5 s^{-1}) is much slower than the practical used shear rate (10^{12} to 10^{14} s^{-1}) in magnetic recording disks. In this study, we investigated the effect of the side chain in a highly confined thin film of Demnum,[24] Krytox,[23] Fomblin Y,[22] and Fomblin Z[22] type perfluoropolyether molecules within the shear rate range of practical use for magnetic recording disks. We examined the difference in the shear rate dependence for the viscosity and film structure between linear and branched molecules. The origin of the difference in the frictional behavior was also analyzed. Further, we investigated whether linear molecules are easily solidified or not.

2. Molecular Model and Simulation Methods

2.1. Molecular Model. The simulation system represents a thin film composed of perfluoropolyethers confined by Ni surfaces as shown in Figure 1. The consistent valence force field (CVFF) developed by Dauber-Osguthorpe et al.[26] in the following form is used for perfluoropolyethers:

$$U_{\text{pot}} = \sum_b H_b(b - b_0)^2 + \sum_\theta H_\theta(\theta - \theta_0)^2 + \sum_\phi H_\phi[1 + s\cos(n\phi - \phi_0)] + \sum_i \sum_{j>i} \left[\frac{A_{ij}}{r_{ij}^{12}} - \frac{B_{ij}}{r_{ij}^{6}} + \frac{q_i q_j}{r_{ij}}\right] + \sum_\chi H_\chi \chi^2 + \sum_b \sum_{b'} F_{bb'}(b - b_0)(b' - b_0') + \sum_\theta \sum_{\theta'} F_{\theta\theta'}(\theta - \theta_0)(\theta' - \theta_0') + \sum_\theta^{\chi} \sum_b F_{\theta b}(\theta - \theta_0)(b - b_0) + \sum_\phi F_{\theta\theta'\phi}\cos\phi(\theta - \theta_0)(\theta' - \theta_0') + \sum_\chi \sum_{\chi'} F_{\chi\chi'}\chi\chi' \quad (1)$$

The first five terms in the equation represent, in this order, the potentials of stretching of bonds, bending of bond angles, torsion angles, van der Waals interactions (Lennard−Jones) and electrostatic interactions (Coulomb), and out-of-plane. The remaining five terms are cross potentials which represent interactions between the former five potential terms. In these simulations, since the influence of the cross terms is sufficiently small, they were ignored. The parameters used are summarized in Table 1. There is some possibility that long molecules do not attain equilibrium on a nanosecond time scale and the cell size (17.842 nm^2) is not large enough for long molecules. Accordingly, short molecule simulations were also carried out. The following long and short molecules were used:

Demnum type: $CF_3CF_2O-(CF_2CF_2CF_2O)n\text{-}CF_2CF_3$, $n = 14, 4$

Krytox type: $CF_3CF_2O-(CF(CF_3)CF_2O)n\text{-}CF_2CF_3$, $n = 9, 4$

Fomblin Z type: $CF_3CF_2O-(CF_2CF_2O)m\text{-}(CF_2O)n\text{-}CF_2CF_3$, $m = n = 14, 3$

Fomblin Y type: $CF_3CF_2O-(CF(CF_3)CF_2O)m\text{-}(CF_2O)n\text{-}CF_2CF_3$, $m = n = 14, 3$

Demnum type ($n = 14$) and Krytox type ($n = 9$) have the same bulk viscosity, $7.4-7.8 \times 10^{-2}$ Pa·s, at 300 K experimentally. If the films are thick and Newtonian liquid, it is well-known that the shear stresses of the films that have the same viscosity are the same. To investigate the thin confined effects on shear stress, the fact that viscosities of Krytox and Demnum long types are the same was used. However, concerning Fomblin Z and Fomblin Y types and short molecules, since there are no experimental data available for which these molecules have the same viscosity, the number of backbone atoms of the molecules was set to the same. The numbers of molecules were set as 17 (Demnum type: $n = 14$); 47 (Demnum type: $n = 4$); 24 (Krytox type: $n = 9$); 47 (Krytox type: $n = 4$); 54 (Fomblin Z type: $m = n = 3$); 54 (Fomblin Y type: $m = n = 3$); 17 (Fomblin Z type: $m = n = 14$); 17 (Fomblin Y type: $m = n = 14$) molecules, so that the cell height was almost the same in all systems. Concerning Fomblin Y and Z, the ratio of n to m of manufactured products differs with molecular weight but is usually under 1.0.

The thin film was confined by two rigid walls of (111) surfaces of fcc Ni lattice composed of two layers. Since CVFF parameters of Ni have not been developed, the interactions between the thin film and Ni surfaces were described by the Lennard−Jones (L−J) potential. These values were derived from the adhesive energy and lattice constant of Ni as follows:[27]

$$U_{ij}(r) = \frac{C_{ij}}{r_{ij}^{12}} - \frac{D_{ij}}{r_{ij}^{6}} \quad (2)$$

where

$$C_{ij} = 4\epsilon_{ij}\sigma_{ij}^{12} \quad (3)$$

$$D_{ij} = 4\epsilon_{ij}\sigma_{ij}^{6} \quad (4)$$

and $\epsilon_{ij} = E$ (adhesive energy)/6 = 71.39 kJ/mol; $\sigma_i = 2^{-2/3}$a (lattice constant) = 0.2217 nm. Kong combining rules ($A_{ij} = (A_{ii} \times A_{jj})^{1/2}$, $B_{ij} = (B_{ii} \times B_{jj})^{1/2}$, $C_{ij} = (A_{ii} \times C_{jj})^{1/2}$, $D_{ij} = (B_{ii} \times D_{jj})^{1/2}$)[26,28] were used. These Ni parameters probably do not

TABLE 1: List of Potential Parameters

atom type	A_{ii} (kJ/mol^{-1} nm^{12})	B_{ii} (kJ/mol^{-1} nm^{6})	mass (amu)
C	0.8294257×10^{-5}	0.4714328×10^{-2}	12.011150
F	0.8419906×10^{-6}	0.9847354×10^{-3}	18.998400
O	0.1142556×10^{-5}	0.2088706×10^{-2}	15.999400

bond	H_b (kJ nm^{-2})	b_0 (nm)
C−C	135114.651144	0.152600
C−F	207665.280000	0.136300
C−O	114383.376000	0.142500

angle	H_θ (kJ mol^{-1} rad^{-2})	θ_0 (deg)
C−C−C	195.104880	110.5000
C−C−F	414.493200	107.8000
F−C−F	397.746000	107.8000
C−C−O	293.076000	109.5000
C−O−C	251.208000	109.5000
C−O−F	397.746000	107.8000
O−C−O	293.076000	109.5000

torsion	H_ϕ (kJ rad^{-1})	n	ϕ_0 (deg)
* C C *	5.955723	3	0.0000
* C C *	1.63176	3	0.0000

atom type

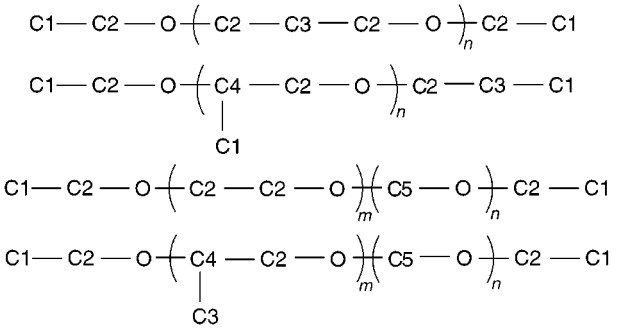

atom type	charge (e)	atom type	charge (e)
C1	0.5338	C5	0.5500
C2	0.4529	O	−0.1941
C3	0.3559	F	−0.1779
C4	0.2750		

cross term	$F_{bb'}$, $F_{\theta\theta'}$, $F_{b\theta}$, $F_{b\theta\phi}$	were set to zero.

represent the precise interactions between perfluoropolyether molecules and the Ni surface, but in these simulations we do not stress the Ni character, so using these parameters is reasonable.

2.2. Simulation Methods. In all cases, the initial conformations were generated between two surfaces by the method which was developed by Theodorou and Suter[29] and has been widely used for constructing well-relaxed amorphous glassy polymers. Accordingly, in each step of the conformation generation, the modified rotational isomeric state conditional probabilities were considered as follows:

$$q'_{\zeta\xi;i} = q_{\zeta\xi;i} \frac{\exp\left[-\dfrac{\Delta U_{\xi;i}}{RT}\right]}{\sum_{\xi'} q_{\zeta\xi';i} \exp\left[-\dfrac{\Delta U_{\xi';i}}{RT}\right]} \qquad (5)$$

where i is the bond generation number, ξ is the rotational state of the bond i, $q_{\zeta\xi;i}$ is the probability for rotational state ξ of bond i when the previous bond state $i-1$ is ζ and $\Delta U_{\xi;i}$ is the increase in long-range interaction energy (the interactions which are not considered when the probability $q_{\zeta\xi;i}$ is determined) in the rotational state ξ. In this process, initial positions of the molecules were randomly generated. The initial densities of each liquid, Demnum long and short molecules, Krytox long and short molecules, Fomblin Z long and short molecules, Fomblin Y long and short molecules, were set as 1.86 and 1.83, 1.87 and 1.83, 1.86 and 1.82, 1.88 and 1.84 g/cm^3, respectively; these are experimental values at room temperature and 0.1 MPa. The films were equilibrated under 4 MPa and 40 MPa for 200−400 ps.

In this study, two types of simulations were performed: (A) The slider was moved in the x axis direction at a constant velocity. (B) The slider was moved periodically in order to measure the viscoelasticity. In the latter, the slider was moved periodically at $x(t) = A \sin(2\pi t/T)$ and the elasticity and viscosity were calculated from the shear response (σ) as follows:[30]

$$\sigma = \sum_{n=1,\text{odd}} (G_n'\gamma^n \sin n\omega t + G_n''\gamma^n \cos n\omega t) \qquad (6)$$

$$G_n^* = G_n' + iG_n'' \qquad (7)$$

where γ is the strain amplitude and G_n' and G_n'' are storage and loss moduli, respectively. The shear stress was calculated as necessary force per unit area to move the slider at a constant velocity.

The slider was moved at a constant velocity mainly 1, 5, 25, 100, or 400 m/s or periodically $x(t) = A \sin(2\pi t/T)$, $A = 0.2-0.5$ nm, $T = 40-60$ ps under constant pressure or constant volume. In simulation (A), the constant volume (NTV ensemble) and constant pressure (NTP ensemble) simulations were carried out at 40 MPa. In simulation (B), constant volume simulations were carried out at 4 MPa and 40 MPa. In the constant pressure simulation, the constant load (40 Mpa) was applied to the slider in the z direction perpendicular to the slider, the same as done in ref 20. The slider movement was determined by a sum of the normal force to the slider surface and the load. The shake algorithm[31] was used in only simulation A, because the fluctuation of the shear stress increases with the shake algorithm and the phase of shear response is sensitive to noise. The time step in the equilibrium condition and the sliding step with the constant velocity 1, 5, 25, 100, or 400 m/s were set to 1.0, 2.0, 1.5, 1.0, 1.0, or 1.0 fs, respectively. Two-dimensional periodic boundary conditions were imposed in the xy plane. The cut off length of nonbonded interactions was set to 0.9 nm. A leapfrog algorithm was used to integrate Newton's equations of motion.[32] The temperature was kept at 300 K by applying Berendsen's thermostat[33] only on the y and z velocity components, since it was difficult to extract the thermal part of the velocity in the sliding direction. Some researchers have adopted the method of thermostating the walls only.[17−19,34] If it were assumed that the wall atoms were attached to a lattice site with a spring to maintain a well-defined solid structure and only the walls were thermostated, at slider velocities faster than about 200 m/s, the temperature would not be controlled completely because heat generation by friction would be too much. Accordingly, the film was thermostated in order to investigate the shear rate dependence of the film properties by keeping the same temperature.

The simulations were performed for 800 ps to 6ns in each case.

3. Results and Discussion of Demnum Type and Krytox Type Molecules

3.1. Constant Volume Simulations. *3.1.1. Shear Rate Dependence of the Film Structures.* The averaged densities of

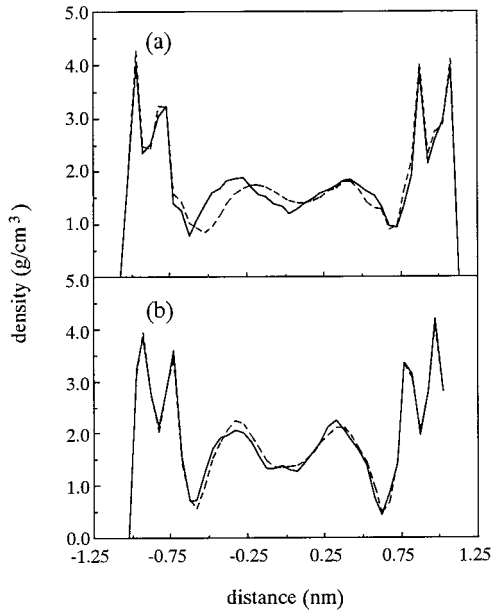

Figure 2. Comparisons of density profiles of films as a function of the distance from the center of the film. The solid and dotted lines represent densities at 1 m/s and 400 m/s slider velocities, respectively. (a) Krytox short type; (b) Demnum short type.

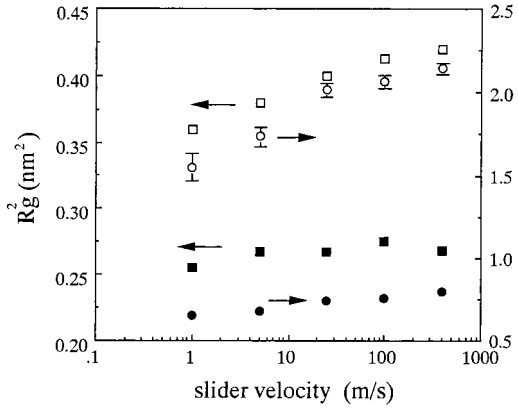

Figure 3. The slider velocity dependence of the squared radius of gyration. R_g^2 of Demnum long and short molecules are open circles and open squares. Those of Krytox long and short molecules are filled circles and filled squares.

Demnum long and short molecules, Krytox long and short molecules after equilibration at 40 MPa without shear are 1.93 and 1.90, 1.93 and 1.90 g/cm^3, respectively. These values of long molecules are in good agreement with experimental values under the same conditions. No comparison for short molecules was possible owing to a lack of their experimental results. Figure 2 shows the density profiles of short Krytox and Demnum molecules. There are almost no differences between low and high shear rates in both cases. This has been reported previously and indicates that the influence of the wall is strong even under high slider velocity.[18,35] The density profiles of Demnum molecules more clearly show the stratified structure than the profiles of Krytox molecules do. This tendency is also found in longer molecules.

As a measure of molecular size, Figure 3 shows the slider velocity dependence of the squared radius of gyration of the molecules (R_g^2). For clarity, error bars are shown only for Demnum long type results. All four molecule types show squared radius of gyration increases with increasing slider velocity. In fully flexible planar Couette flow with constant volume, linear normal alkane molecules stretched and lined up

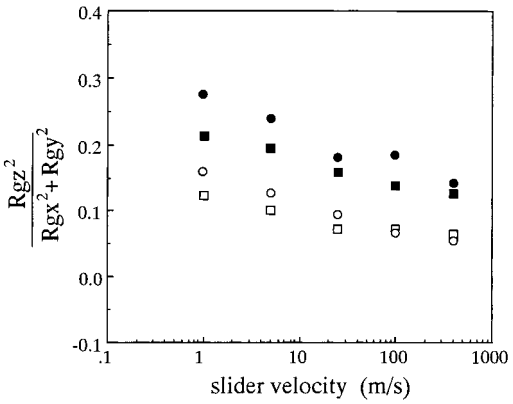

Figure 4. The slider velocity dependence of anisotropy of the molecules $2R_gz^2/(R_gx^2 + R_gy^2)$. R_gx is the radius of gyration of the molecules in the x axis direction. The anisotropies of Demnum long and short type molecules are open circles and open squares. Those of Krytox long and short molecules are filled circles and filled squares.

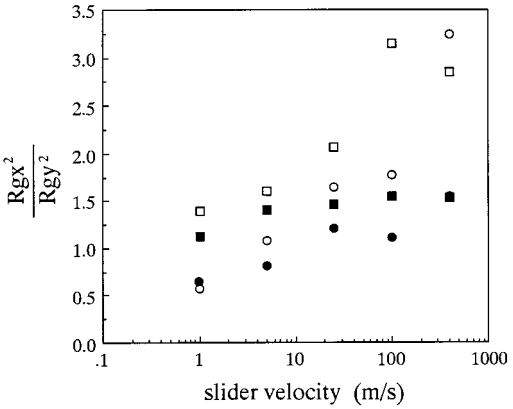

Figure 5. The slider velocity dependence of anisotropy of the molecules' R_gx^2/R_gy^2. Anisotropy of Demnum long and short molecules are open circles and open squares. Those of Krytox long and short type molecules are filled circles and filled squares.

at lower shear rates and coiled up at higher shear rates. Accordingly, they had the maximum R_g.[15,36,37] However, in our present simulations, at least at these shear rates, there is no maximum. This is presumably because, for higher shear rate, the torque becomes larger and compact conformations become stable for molecules when the film is thicker than a certain value or under planar Couette flow with constant volume. However, our films are sufficiently thin, since the molecules are influenced by both the slider and base, and the stretched conformations are stable independent of shear rate.

We show the anisotropy of the molecules in Figures 4 and 5. The molecules flatten and lengthen in the sliding direction. This tendency is very remarkable in the Demnum type. As shown in Figure 6, we investigated the molecular order using the order parameter defined as the largest eigenvalue of the ordering matrix Q:[38]

$$Q_{\alpha\beta} = \frac{1}{2N}\sum_i (3e_{i\alpha}e_{i\beta} - \delta_{\alpha\beta}), \quad \alpha, \beta = x,y,z \tag{8}$$

where $e_{i\alpha}$ represents the unit vector element of the ith bond of the main chain in each molecule and N is the number of the bonds. For clarity, error bars are shown only for Demnum long type results. Figure 6 shows that order parameters of the Demnum type are higher than those of the Krytox type and that slider velocity dependence of the Demnum type (linear) is higher than that of the Krytox type (branched). These results

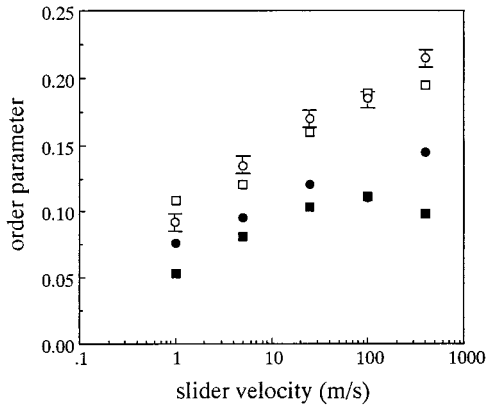

Figure 6. The slider velocity dependence of the order parameter. The order parameters of Demnum long and short molecules are open circles and open squares. Those of Krytox long and short molecules are filled circles and filled squares.

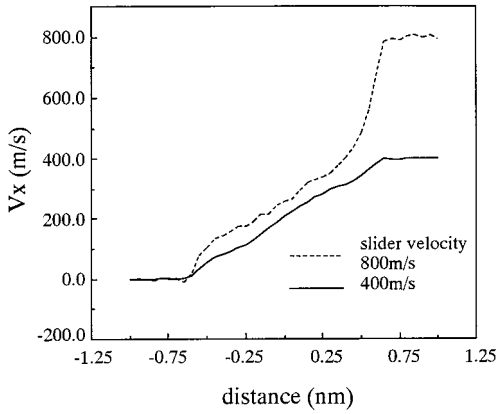

Figure 7. The averaged velocity of the Krytox long type as a function of the distance from the center of the film.

indicate that the linear molecules tend to deform and line up in the sliding direction more easily than branched molecules. The side chains are expected to prevent the molecules from ordering. These tendencies are essentially identical to those obtained with hydrocarbons.[14,18]

3.1.2. Comparison of the Viscosities. The *x* component (sliding direction) of velocity of the molecules as a function of the distance from the center of the film of Krytox long molecules is plotted in Figure 7 with slider velocities of 400 m/s and 800 m/s. The 800 m/s slider velocity curve at 0.5−0.7 nm shows that the interlayer slip occurs between the molecules closest to the slider and the inner molecules. The interlayer slips of Demnum long and short, Krytox long and short molecules begin at about 550 and 450, 400 and 350 m/s, respectively. The shear stresses at these velocities are 341 (± 11) and 266 (± 8), 286 (± 9), and 243 (± 8) MPa, respectively. At slider velocities above the critical velocity at which interlayer slip begins, the shear stress does not increase clearly. That is, this is the maximum shear stress which the molecules can transmit to other molecules as reported previously.[44] The interlayer slips[20,21,45] and the relationship between the amount of slip and the shear rate[46] have been studied extensively. If the slider velocity were faster than about 400 m/s, the temperature would not be controlled completely because heat generated by the friction would be too much. Accordingly, to confirm this tendency, simulations under 4 MPa were also carried out. The interlayer slips of Demnum long, Krytox long molecules begin at about 400, 300 m/s and the shear stresses are 296 (± 8), 267 (± 8) MPa, respectively. The maximum shear stress is thought to be

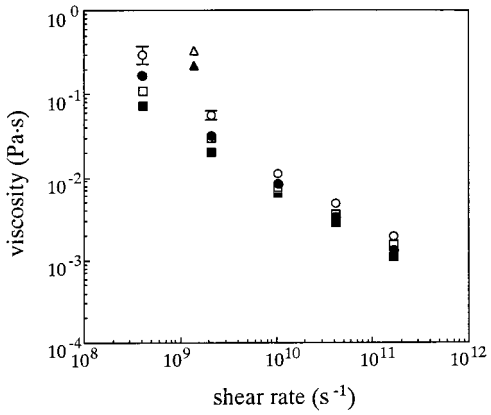

Figure 8. The apparent shear rate dependence of viscosity of Demnum and Krytox types at 40 MPa and 4 MPa. The open squares and open circles represent viscosities of Demnum short and long type molecules at 40 MPa, respectively. The filled squares and filled circles represent viscosities of Krytox short and long type molecules at 40 MPa, respectively. The open and filled triangles represent Demnum long and Krytox long molecules at 4 MPa, respectively.

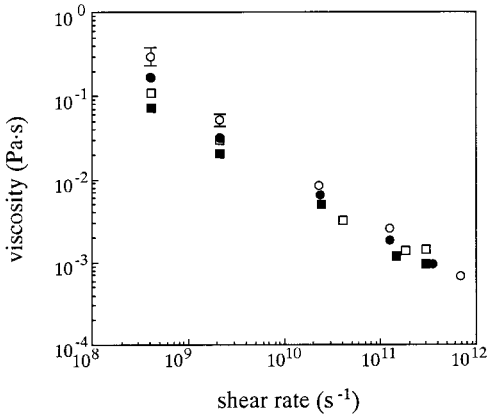

Figure 9. The actual shear rate dependence of viscosity of Demnum and Krytox types at 40 MPa. The open squares and open circles represent viscosities of Demnum short and long molecules, respectively. The filled squares and filled circles represent viscosities of Krytox short and long molecules, respectively.

higher in branched molecules than in linear molecules, because side chains are expected to become interwined with each other. However, the result is the opposite. Each system with 25−400 m/s slider velocities, except for Krytox short type 400 m/s, shows discontinuous velocities similar to the 400 m/s velocity curve at ±0.6 nm in Figure 7. The discontinuity of the velocity is unclear when the slider velocity is 1 m/s or 5 m/s. This indicates that the actual shear rate is different from the apparent shear rate as the slider velocity is divided by the film thickness. Hereafter, we distinguish them as actual shear rate and apparent shear rate. Figures 8 and 9 show log−log plots of viscosities against apparent shear rate and actual shear rate, respectively. For clarity, error bars are shown only for Demnum long type results. The viscosity is calculated as the shear stress divided by apparent or actual shear rate. No significant difference is observed between the figures. Since there are no experimental data available at 40 MPa, the viscosities at 4 MPa, which is closer to the experimental condition, are also plotted for comparison. However, these shear rates are higher than the reported experimental values 10^{-2} to 10^{4} s^{-1} and these experiments were carried out for a constant load (constant pressure).[11] These figures show power law behavior in all cases. In SFA experiments, Demnum and Krytox, which have the same molecular weight as Demnum and Krytox long molecules in

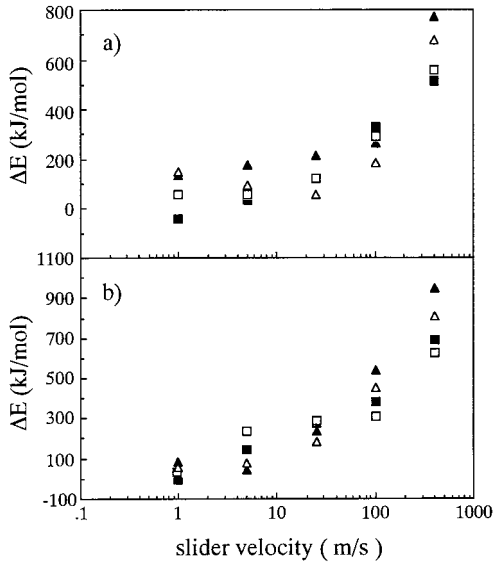

Figure 10. The slider velocity dependence of inter- and intramolecular nonbonded energy differences (ΔE) under shear and equilibrium state. The filled squares and triangles represent intra- and intermolecular nonbonded energy differences of Krytox molecules. The open squares and triangles represent those of Demnum molecules. (a) Short molecules; (b) long molecules.

these simulations, show shear thinning, that is, the viscosity decreases with increasing shear rate, and the power law exponent is −1.0 to −0.80 at low load around 10 MPa.[11] The power law exponents in both Figures 8 and 9 are about −0.75 to −0.80 which are close to the experimental exponents with constant pressure. In some previous simulations of hydrocarbons, the power law exponent of branched molecules was larger than that of linear molecules.[14−16] In our simulations, when the actual shear rate is used, the power law exponent of Krytox type (branched) is somewhat smaller than that of Demnum type (linear) in long molecules.

In the SFA experiments of Demnum and Krytox long molecules, the effective viscosities of branched molecules are considerably lower than those of linear molecules within the linear response region under periodic shear. In the nonlinear response region, although the viscosities were not discussed in the text, the viscosity of Demnum molecules at zero shear rate with 4 MPa is about $10^{5.9}$ Pa·s and that of Krytox molecules is about $10^{5.7}$ Pa·s in the confined thin film condition in the graph in the paper.[11] The calculated viscosities at 4 MPa in Figure 8 are regarded as reasonable results considering the power law exponent. The viscosities of Demnum type (linear) are higher than those of Krytox type (branched) in short chains at each given shear rate in Figures 8 and 9, except the highest shear rate in Figure 9. In the shear simulation of hydrocarbons, the shear viscosity of linear molecules is almost the same as that of branched molecules when the side chain is single and short[16] and is smaller than that of branched molecules when the side chains are multiple or long.[15,19] In contrast, our simulation results reveal that the shear viscosity of linear molecules (Demnum type) is higher than that of branched molecules (Krytox type) with multiple side chains in perfluoropolyethers, although their bulk viscosities are the same or the numbers of backbone atoms are the same and bulk viscosities under shear without walls are almost the same.[47]

3.1.3. Potential Energy Properties under Shear. To investigate how a film changes from the viewpoint of potential energy, the energy difference of the nonbonded energy (L−J + electrostatic) under shear and in the equilibrium state are plotted. Figure 10 reveals that for both short and long molecular lengths, the difference of intermolecular nonbonded energy of Krytox type at higher slider velocity is somewhat larger than that of the Demnum type, while the difference of intramolecular nonbonded energy is almost the same. Figure 11 shows the slider velocity dependence of the difference of bending angle energy under shear and in the equilibrium state. In long molecules, the difference for Krytox type is larger than that of the Demnum type at higher slider velocity. The difference of dihedral angle energy has almost the same tendency as bending angle energy. These findings indicate that when there is a side chain the film has a less ordered conformation under shear as represented by the order parameters and this causes intermolecular strain at higher slider velocity.

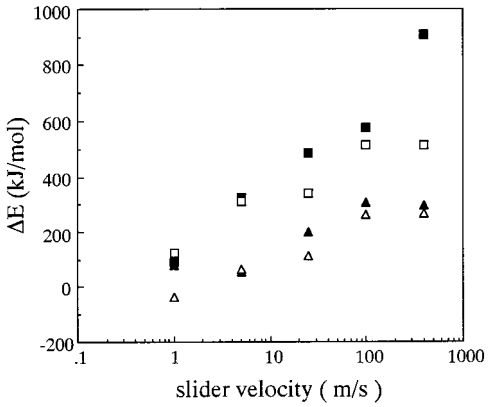

Figure 11. The slider velocity dependence of the bending angle energy differences (ΔE) under shear and equilibrium state. The open squares and open triangles represent ΔE of Demnum long and short molecules, respectively. The filled squares and filled triangles represent ΔE of Krytox long and short molecules, respectively.

Shear thinning means that the required energy for the slider to move per distance becomes smaller than the values expected from Newton's law of viscosity on increasing the slider velocity. Shear thinning occurs when the shear rate is higher than the inverse of the longest molecular relaxation time,[30] and this has been confirmed by experiments[7] and simulations.[21,43] Although the molecular order under higher shear rate is considered to cause the shear thinning, the molecular order difference of films at different shear rates is not clearly observed sometimes, e.g., the Krytox type at higher shear rate in Figure 6. To investigate how the environment of the molecules is changed with the slider velocity (or shear rate), the intermolecular nonbonded interactions (L−J + electrostatic) as a function of sliding distance of the slider between an atom and atoms of other molecules and between a molecule and other molecules were investigated. Slider velocity dependence of the intermolecular interaction, as a function of the sliding distance of the slider for a molecular unit (a molecule and other molecules), is not observed. Possibly, any difference between the intermolecular interaction for a different sliding velocity is canceled by the multiple atoms in a molecule. However, dependence of the interaction for an atomic unit (an atom and other atoms which belong to other molecules) is observed as shown in Figure 12. Here, the atom which is almost in the center of the film thickness is chosen. Figure 12 shows that, with increasing velocity, the long distance periodic changes (of the nonbonded interaction between an atom and other atoms) increase and short distance periodic changes decrease.

Figure 13 shows the power spectra of the nonbonded interaction between an atom and other atoms of the other molecules as a function of sliding distance for different sliding

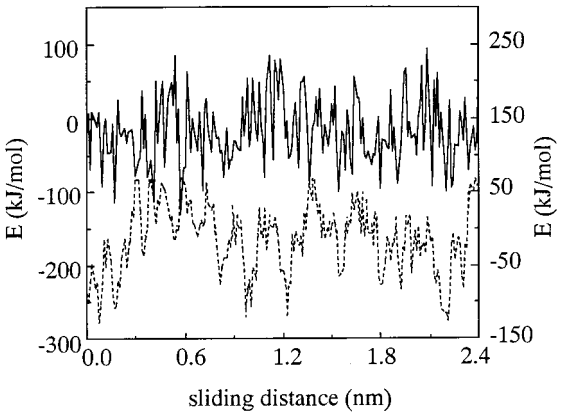

Figure 12. The nonbonded interaction between an atom and other atoms of other molecules of Krytox short type as a function of the sliding distance of the slider. The solid and dotted lines represent those of 25 m/s and 400 m/s slider velocities, respectively.

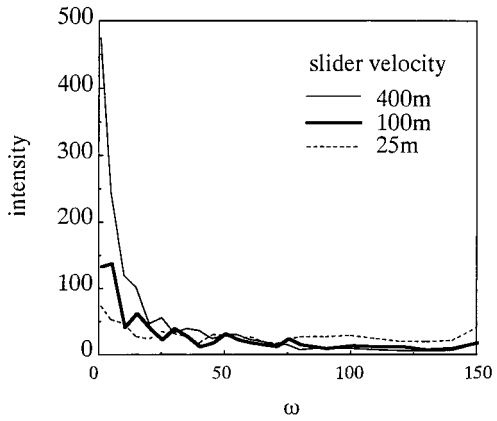

Figure 13. The power spectra of nonbonded interaction between an atom and other atoms of Krytox short molecules as a function of a sliding distance ($\omega = \pi/4$ rad/nm) for different sliding velocities. The power spectra were five-averaged for smoothing.

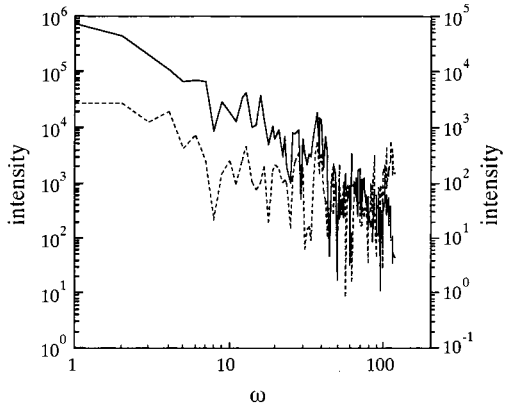

Figure 14. Comparison of the power spectrum of shear stress (dotted line) and the power spectrum of total potential energy (solid line) of Demnum long molecules with 400 m/s slider velocity against frequency ($\omega = 2\pi/500$ rad/ps).

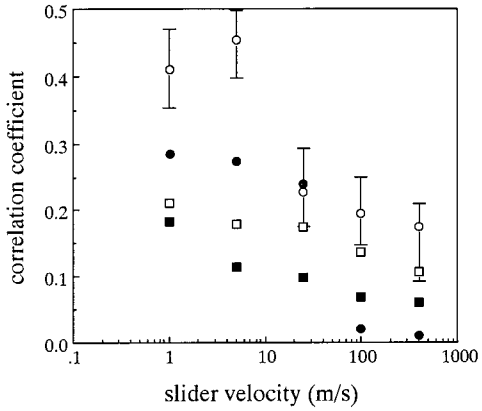

Figure 15. The slider velocity dependence of the correlation coefficient between shear stress and total potential energy of the system. The open squares and open circles represent Demnum short and long molecules, respectively. The filled squares and filled circles represent Krytox short and long molecules, respectively.

velocities. This figure clarifies the tendency we noted above, that is, short distance periodic energy changes decrease and long distance periodic energy changes increase with increasing slider velocity. The power spectrum of temporal frequency also shows higher intensities at low frequencies at faster shear rate. The same tendencies are observed in other atoms at a different position from the walls and for other molecular types. However, this difference is not clear between 5 and 1 m/s slider velocities, because the energy changes are buried in the thermal fluctuations. The required energy for an atom to pass the certain distance is expected to decrease with increasing slider velocity due to the decrease of the short periodic energy change, because the sum of the increasing part of the periodic energy change becomes smaller with the decrease of short periodic energy change. Accordingly, the decrease of short periodic energy change is expected to be one of the causes of shear thinning.

3.1.4. Correlation between Each Energy and Shear Stress. The SFA experimental results showed that the friction increased steadily over repetitive cycles and collapsed intermittently to the average value. Further, it was reported that the squared amplitudes of the Fourier components of the frictional force against frequency showed power law decay.[39] That is, the friction did not always have an exact value. In our simulation also, the shear stress has about a 10−20% uncertainty with some periodicity. Figure 14 shows the power spectrum of shear stress of long Demnum molecules (400 m/s slider velocity). The high frequency effects are large, and shear stress decreases only at low frequencies, but no convincing power law decay is observed, probably because the sliding velocity is too fast. We need to consider how the film potential energy changes with fluctuations of shear stress. Figure 15 shows the correlation coefficient between shear stress and total potential (film + interfacial) energy of the systems as a function of the slider velocity. For clarity, the error bars were shown only for the long Demnum type results. The correlation coefficient was calculated as follows:

$$C_{XY} = \frac{<X(t) - \bar{X}><Y(t) - \bar{Y}>}{<(X(t) - \bar{X})^2>^{1/2}<(Y(t) - \bar{Y})^2>^{1/2}} \qquad (9)$$

where X and Y are physical quantities, $\bar{X}$ is the averaged value, and $<>$ mean ensemble average. The correlation coefficients are low for all cases and there is no apparent correlation between shear stress and total potential energy of the system. The correlation coefficients between shear stress and each energy term such as nonbonded interaction energy, bending angle energy, and interfacial interaction (between the slider or base and the film) are also low, and there is no apparent dependence on slider velocity. However, if we assume that the shear stress becomes large for the slider and the film to pass over unstable conformations (high energy points), when the strain energy becomes higher than a critical value, a time lag between strain energy and shear stress is expected. If there is a time lag between

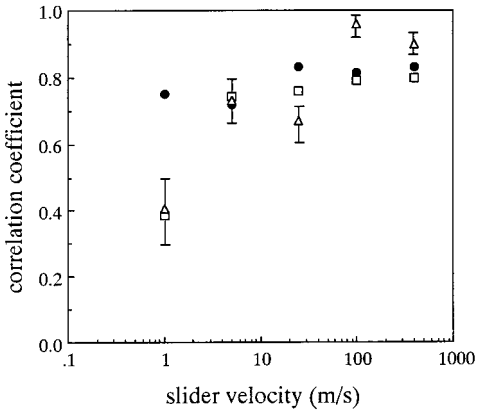

Figure 16. The correlation coefficient at low frequencies (1−40 ω, $\omega = 2\pi$ rad/ns; faster than 25 m/s slider velocity, $\omega = \pi$ rad/ns; others) between power spectra of shear stress and each energy in the long Demnum type. The squares, filled circles, and triangles represent correlation coefficients between shear stress and interfacial interaction energy (between slider and the film), those between shear stress and nonbonded film energy, and those between shear stress and total potential energy of the system, respectively.

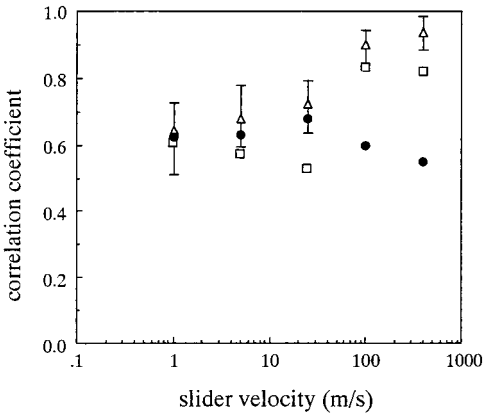

Figure 17. The correlation coefficient at low frequencies (1−40 ω, $\omega = 2\pi$ rad/ns; faster than 25 m/s slider velocity, $\omega = \pi$ rad/ns; others) between power spectra of shear stress and each energy in the long Krytox type. The squares, filled circles, and triangles represent correlation coefficients between shear stress and interfacial interaction energy (between slider and the film), nonbonded film energy, and total potential energy of the system, respectively.

shear stress and strain energy or if shear stress and/or strain energy include noise, the relationship is not recognized by this correlation coefficient. So the power spectrum of the total potential energy was calculated and also shown in Figure 14. The power spectrum of total potential energy and the pattern of the power spectrum is comparatively similar to the power spectrum of the shear stress at low frequencies, but the power spectrum of the total potential energy is smaller than that of shear stress at high frequencies. Concerning Figure 14, the correlation coefficients of the power spectra of total potential energy and that of shear stress in the range of 1−40 ω and 40−2000 ω are 0.89 (± 0.03) and 0.22 (± 0.15), respectively. This means that the low frequency change of the shear stress is accompanied by the total potential (film + interfacial) energy change, while the high frequency change of the shear stress is not accompanied by it; probably high frequencies are due to thermal fluctuations and noise. Further, the correlation coefficients of real parts of the Fourier components of shear stress and those of total energy and the correlation coefficients of the imaginary parts of them are 0.80 (± 0.04) and 0.92 (± 0.04), respectively. This indicates that there is no time lag between shear stress change and total energy change and that the correlation coefficients in Figure 15 are low because of the high-frequency part of the shear stress. These correlation coefficients suggest that when the strain energy of the film becomes high, the shear stress becomes large for the slider and the film to pass over the unstable conformation.

To get further insights into the correlation between shear stress and each potential energy and slider velocity dependence of the correlation between them, correlation coefficients of the power spectrum at low frequencies (1−40 ω) of shear stress and the power spectra at low frequencies of the interfacial interaction (between the slider or base and the film), those between shear stress and nonbonded interaction, and those between shear stress and total potential energy of the system (film energy + interfacial interaction) in Demnum and Krytox long types are investigated as shown in Figures 16 and 17. For clarity, error bars are shown only for total potential energy results. The Demnum and Krytox short types also show the same tendencies as the long molecules. Further, the correlation coefficients of each real and each imaginary part of the Fourier components are also almost the same as those of the squared amplitude of the Fourier components within 0.1 error bars, that is, no time lag is observed between them. The correlation coefficients between the power spectrum of the total system potential energy and that of the shear stress are high and independent of slider velocity in both figures. This indicates that the low frequencies shear stress change has the same relationship with potential energy as the film (system) strain. That is, when the strained energy of the system is large, the shear stress becomes large for the slider and film to pass over the unstable point (high energy point). This tendency is remarkable at higher slider velocity, probably because the molecules cannot avoid the unstable point (high energy point), since the slider velocity is too fast. Figures 16 and 17 also show that the correlation coefficients between the power spectrum of nonbonded interaction (L−J + electrostatic) and that of shear stress are high. The correlation coefficients of power spectra between shear stress and bending angles or dihedral angles also show the same tendency for nonbonded interaction. That is, every energy term has some relationship with shear stress fluctuation; it is not that only a specific term has a relationship with shear stress fluctuation. Further, Figure 17 shows that correlation coefficients of the power spectra between nonbonded interaction and those of shear stress are somewhat smaller than those of the Demnum type (Figure 16), and they decrease slightly with faster slider velocity. The lower correlation coefficients of the power spectra of nonbonded interaction and those of shear stress in Krytox than in Demnum are interpreted as follows. The shear stress of two surfaces sliding (for example, a slider surface and a film surface) has long been recognized to be dominated by the adhesion (interfacial) energy between them in many cases;[40] recently, it has come to be recognized as dominated by adhesion hysteresis.[41,42] When the array of molecules closest to the surface changes, interfacial interaction also changes, causing the shear stress and nonbonded energy to change. In the Demnum type, since the film is well-ordered, the film changes cooperatively with the interfacial energy change. In the Krytox type, since the film is less ordered, only a part of the film changes cooperatively with the interfacial energy change. With faster slider velocity, this tendency becomes significant and only the closest molecules change, and the correlation coefficients of the power spectrum of nonbonded energy of the film and that of shear stress decrease and those of interfacial and shear stress increase as shown in Figure 17. This behavior is expected to be the one of the causes of the

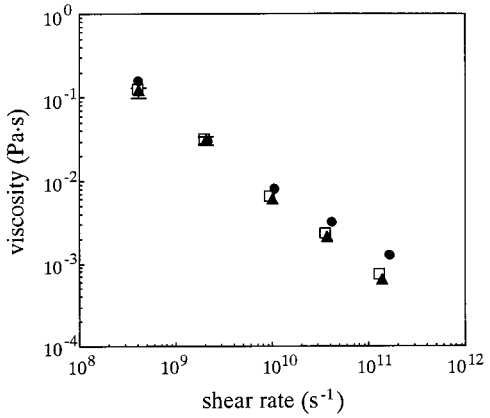

Figure 18. The apparent shear rate dependence of viscosities of Demnum short type (open squares), Krytox short type (filled triangles) under constant pressure and Krytox short type (filled circle) under constant volume.

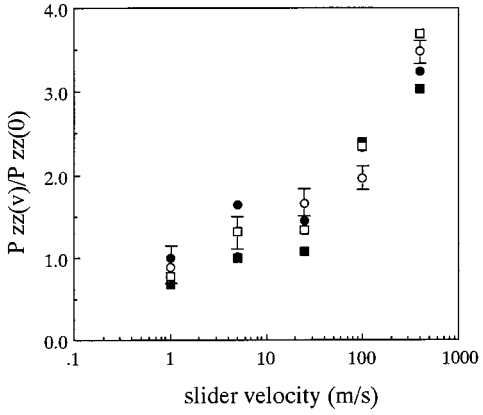

Figure 19. The slider velocity dependence of the *P*zz(v) divided by the *P*zz(0) at equilibrium. The open squares and open circles represent *P*zz(v)/*P*zz(0) of Demnum short and long molecules, respectively. The filled squares and filled circles represent those of Krytox short and long molecules, respectively.

lower viscosity and lower maximum shear stress of the Krytox type.

3.2. Constant Pressure Simulations. *3.2.1. Comparison of the Viscosities.* Figure 18 shows the viscosities under constant pressure of Demnum and Krytox short types against the apparent shear rate with those of the Krytox type under constant volume as a comparison. The trend of viscosity against the actual shear rate is almost the same as that of the apparent shear rate (Figure 18). The power law exponents are −0.8 to −0.85 which is in agreement with experimental values (−0.8 to −1.0)[11] and smaller than that of the constant volume simulation in 3.1.2. The viscosities of the molecules under constant pressure are smaller than those under constant volume in this shear rate range. These phenomena have also been observed and discussed in previous confined simulations[21,43,45] and in Couette flow simulations.[36] This is simply because the distance between two walls becomes larger with slider velocity higher than 5 m/s. The wall−wall distance deviations from the equilibrium condition (about 2.5 nm in the Krytox type and 2.4 nm in the Demnum type) are 0.40, 0.31, 0.14, 0.04, 0.02 nm in Krytox types, and 0.35, 0.26, 0.13, 0.02, 0.02 nm in Demnum types, with slider velocities of 400 m/s, 100 m/s, 25 m/s, 5 m/s, 1 m/s. The decrease of density with increasing shear rate is called "shear dilatancy".[36] In this simulation, the movement of the slider is determined by the pressure, *P*zz, which is calculated as the *z* component of the force from the film to the slider divided by the surface area, and the load as mentioned in section 2.2. Figure 19 shows the slider velocity dependence of *P*zz under constant volume simulations. For clarity, the error bars are shown only for long Demnum type results. It is predicted from the significant increase of *P*zz in this figure that the wall−wall distance is sensitive to the sliding velocity. The increase of the distance of the Krytox type is larger than that of the Demnum type for faster slider velocity under constant pressure simulation, because of the side chain effect. In the constant pressure simulation, the total pressure calculated by the method of plane[48] is almost the same as that of the equilibrium condition. In the constant volume simulations, increased collisions of the slider and film atoms with faster slider velocity cause the increase of pressure of each component. In the pressure constant simulations, the influence from moving the slider is lost by the increase of wall−wall distance. The eigenvalues and R_g^2 under constant pressure are somewhat smaller and larger than those under constant volume at faster slider velocity, respectively. Further, slider velocity dependence of the energy change of each energy term in Demnum and Krytox types is almost the same as that in the constant volume simulation. The Krytox type has more unstable intermolecular interactions than the Demnum type has as in the constant volume simulations in Figure 10 (a).

3.2.2. Correlation between Each Energy and Shear Stress. Under constant pressure simulations, fluctuations of shear stress are also observed. No difference from those of the constant volume simulations is apparent. To clarify the relationship between the change of the wall−wall distance, each energy, and shear stress, the correlation coefficients were investigated and they are listed in Table 2. These correlation coefficients, except for the correlation coefficient between the wall−wall distance and intermolecular L−J energy, are quite low and there is no distinct correlation between them. To exclude the high frequency parts from them, which are not expected to have a relationship with the other terms, the correlation coefficients of the power spectra at low-frequency terms 1−40 ω were investigated as in the previous section and they are listed in Table 3. The correlation coefficients of the imaginary parts of their Fourier components and those of real parts are almost the same values as those of the squared amplitude of Fourier components within 0.1−0.2 errors. The shear stress and wall−wall distance have a relationship which indicates that the slider moves to avoid the high energy (strained) points by changing the slider height (wall−wall distance) rather than passing over them. However, the higher correlation coefficients between the wall−wall distance and total energy and between the distance and inter-L−J indicate that the high energy points are not completely avoided. Based on these slider movements, the correlation between the shear stress and the interfacial interaction between the slider and the liquid film becomes lower under constant pressure compared with those under constant volume in Figures 16 and 17. This is significant in the Demnum type. The frictional mechanism at the surface is expected to change and the surface friction is decreased. These slider movements, to avoid higher energy points, are expected to be one of the causes of the lower shear stress.

3.3. Viscoelastisity of Krytox and Demnum. In SFA experiments, Demnum is observed to have G'(storage moduli) $\gg G''$(loss moduli) in linear shear response and to be easily solidified. In contrast, Krytox is observed to have $G' = G''$ in the frequency ranges $1-10^3$ Hz with 0−4 MPa pressure. In the simulations, G' and G'' of Demnum are 345 (± 16) and 156 (± 12) MPa, and those of the Krytox type are 287 (± 15) and 125 (± 14) MPa, respectively at 4 MPa with constant volume simulations and they are 290 (± 20) and 150 (± 18) MPa, 265

TABLE 2: Correlation Coefficients (with 25 m/s Slider Velocity) between Shear Stress and Wall−Wall Distance, Shear Stress and Interfacial Interaction, Wall−Wall Distance and Total Potential Energy, and Wall−Wall Distance and Intermolecular Nonbonded Interaction

molecular type	shear stress/distance	shear stress/interfacial	distance/total *E*	distance/inter-L−J
Demnum short	0.12 (± 0.05)	0.03 (± 0.04)	0.03 (± 0.05)	0.87 (± 0.06)[a]
Demnum long	0.02 (± 0.07)	0.04 (± 0.06)	0.02 (± 0.07)	0.76 (± 0.06)
Krytox short	0.07 (± 0.05)	0.06 (± 0.05)	0.01 (± 0.06)	0.80 (± 0.06)
Krytox long	0.13 (± 0.08)	0.11 (± 0.09)	0.04 (± 0.08)	0.90 (± 0.07)

[a] Uncertainties are given in parentheses.

TABLE 3: Correlation Coefficients (with 25 m/s Slider Velocity) of Power Spectra at Low Frequencies (1−40 ω, $\omega = \pi$ rad/ns) between Shear Stress and Wall−Wall Distance, Shear Stress and Interfacial Interaction, Wall−Wall Distance and Total Potential Energy, and Wall−Wall Distance and Intermolecular Nonbonded Interaction

molecular type	shear stress/distance	shear stress/interfacial	distance/total *E*	distance/inter-L−J
Demnum short	0.71 (± 0.04)	0.01 (± 0.05)	0.77 (± 0.05)	0.94 (± 0.05)
Demnum long	0.65 (± 0.05)	0.10 (± 0.06)	0.73 (± 0.06)	0.90 (± 0.06)
Krytox short	0.59 (± 0.05)	0.58 (± 0.05)	0.88 (± 0.05)	0.94 (± 0.05)
Krytox long	0.53 (± 0.06)	0.41 (± 0.08)	0.92 (± 0.07)	0.99 (± 0.07)

(± 20) and 218 (± 25) MPa at 4 MPa with constant pressure simulations in the frequency ranges $1.6-2.5 \times 10^{10}$ Hz of linear shear response. At 40 MPa pressure, those of the Demnum type are 371 (± 20) and 218 (± 20) MPa and those of Krytox are 331 (± 19) and 134 (± 16) MPa, with constant volume, respectively. In both cases, there is no obvious difference between Krytox and Demnum types. Further, $G' = G''$ indicates that these films are not solidlike. Although several factors such as slider material difference and compression method difference are expected to contribute to the Krytox type not being solidified, the following interpretation is also reasonable. The solidlike behavior of the Demnum type observed in the experiment is not caused by a solid state but by an entangled effect. In Krytox, τe (longer than τe time, the molecules feel the constraints imposed by the tube) is longer than the inverse of the measured frequency range and then G' is equal to G'' and they are proportional to frequency. Concerning the Demnum type, in contrast, τe is shorter than the inverse of the measured frequency range. Since the inverse of the measured frequency range is between τe and τd (the longest relaxation time), $G' \gg G''$ is observed in Demnum. It is well-known that when the time scale t is $\tau e < t < \tau d$, viscoelasticity of molecules gives $G' > G''$ because of the entangled effect.[30] It has been reported that the dense polyethylene melt of n-$C_{100}H_{202}$ at 500 K does not show the entangled effect.[49] Considering the molecular length of Krytox and Demnum, if they are in the bulk condition, they would not show the entangled effect. However, from SFA experiments for a confined thin film, the entangled effect has been observed in comparatively small molecular weight molecules which would not show the entangled effect in the bulk condition.[50] Probably, Demnum and Krytox show the entangled effect because of the confined thin effect. Unfortunately, τe is longer than the available CPU time and it is impossible to clarify this point by these simulations.

4. Results and Discussion of Fomblin Y Type and Fomblin Z Type Molecules

4.1. Comparison of the Viscosities. It was shown by SFA experiments that the shear stresses of Fomblin Z and Fomblin Y confined conditions are several orders of magnitude larger than their corresponding bulk values, and the effect of confinement on viscosity of Fomblin Z is 10 times larger than that of Fomblin Y.[9] The shear stress of Fomblin Z is also reported to decrease with increasing shear rate as mentioned above. In this section, we investigated shear properties of Fomblin Y type and Fomblin Z type by constant volume simulation.

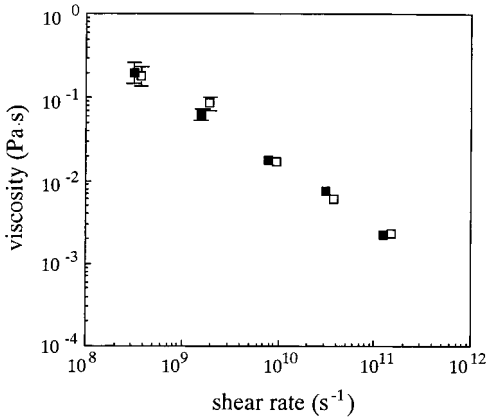

Figure 20. The apparent shear rate dependence of viscosities of Fomblin Y long type (open squares) and Fomblin Z long type (filled squares).

The averaged densities of Fomblin Y long and short molecules, Fomblin Z long and short molecules after equilibration at 40 MPa, are 1.93 and 1.90, 1.93 and 1.90 g/cm^3, respectively. Unfortunately, we could not find the experimental data under the same conditions.

The viscosity of long molecules as a function of the apparent shear rate is plotted in Figure 20. No difference between Fomblin Y and Fomblin Z long types is observed. The power law decays against shear rate and the slope is about −0.7. In Fomblin Y and Fomblin Z short types, the viscosities at a slider velocity of 25 m/s are 1.10 (± 0.15) $\times 10^{-2}$ Pa·s and 1.30 (± 0.2) $\times 10^{-2}$ Pa·s, respectively, and no difference is observed. Further, the critical sliding velocity and shear stress of Fomblin Z and Fomblin Y long types at which the interfacial slips begin are 350 m/s, 326 (± 14) MPa and 320 m/s, 294 (± 12) MPa. The maximum shear stress, which is expected as the maximum value for molecules to transmit to other molecules, of linear molecules (Fomblin Z type) is somewhat larger than that of branched molecules (Fomblin Y type), similar to findings for Demnum and Krytox types. It seems that the critical sliding velocity and the shear stress are decreased by the side chain presence. By comparing the maximum shear stress and the shear viscosity of Demnum, Krytox, Fomblin Y, and Fomblin Z types, no relationship between the maximum shear stress and the viscosity is observed. The maximum shear stress and the critical velocity is expected to be determined by multiple factors, such as molecular length, molecular flexibility, viscosity, etc.

Figure 21 shows the order parameters of the molecules. No difference between Fomblin Y and Fomblin Z types is observed.

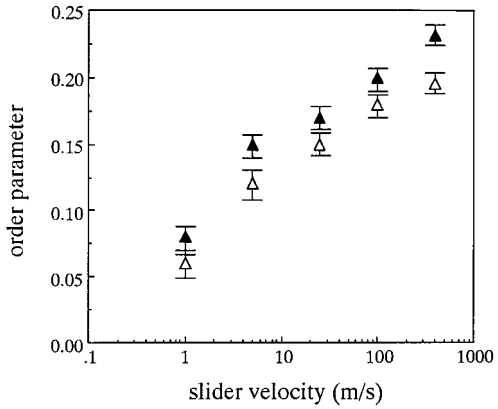

Figure 21. The slider velocity dependence of the order parameter of Fomblin Y long type (open triangles) and Fomblin Z long type (filled triangles).

Further, regarding the increase of each potential energy under shear, no difference is observed between them. Considering the order parameters of the Demnum and Krytox types in Figure 6, the side chains that prevent molecules from ordering cause higher strain energy; however, when the molecules have many ether linkages, they become flexible, the side chain effect decreases, and the molecules tend to order. Molecular order difference is not expected to have a direct influence on viscosity difference. However, absence of the molecular order difference is interpreted as showing that the side chain effect is small enough to have almost the same viscosity in Fomblin Y and Fomblin Z types. Probably because of a dependence on the ratio of ether linkages (the ratio of *n* to *m* in the chemical structure in section 2.1), the film of Fomblin Y has a different character than that of Fomblin Z type.

The difference between Fomblin Y and Fomblin Z types observed in SFA experiments is caused, in part, by the small ratio of *m*/*n* Fomblin Y as noted in section 2.1. However, judging from the results of the Demnum and Krytox types, the fact that the film of Fomblin Y follows Newton's law of viscosity at the shear rate, which is faster than the inverse of the molecular relaxation time, is not expected to be caused by the molecular structure but by the film structure, as discussed by Subbotin et al.[51]

5. Conclusions

We have reported the shear properties of confined perfluoropolyethers. The viscosities of Demnum and Krytox compared reasonably with values estimated from the experiments, and all molecules (Demnum type, Krytox type, Fomblin Y type, Fomblin Z type) showed shear thinning. Power law exponents agreed with observed experimental values. The branched Krytox type showed lower shear viscosities than did those the of linear Demnum type. In contrast, large molecules, Fomblin Y and Fomblin Z types, which have the same number of backbone atoms, had almost the same viscosity. The molecular ordering of the film was higher in the linear Demnum type than in the branched Krytox type. However, differences between branched Fomblin Y type and linear Fomblin Z type were not clearly observed. That is, the side chain prevented molecules from lining up. However, when ether linkages were many and molecules were flexible, the effect of the side chain was small. This molecular order difference was expected to cause the difference between Demnum and Krytox types, and Fomblin Y and Fomblin Z types. The fact that the ordered film showed higher shear rate was contrary to the experimental results of semicrystalline matter observed by Pooley and Tabor.[25] Probably, molecular order was necessary in the semicrystalline state to avoid being caught by the slider surface roughness and the side chains caused the higher shear stress. On the other hand, in a liquid film, the side chains had freedom for the molecules to pass each other, at least when the side chain length was adequate. These were expected to be the causes of the difference between simulation results and experimental results.

The comparisons of nonbonded interaction energy between an atom and other atoms of other molecules as a function of the sliding distance at different slider velocities clarified that the short distance periodic nonbonded interaction energy changes decreased and long periodic energy changes increased with increasing slider velocity. This showed that the potential energy surface (energy environment) an atom feels for a certain distance movement changed with slider velocity. This was probably because of the film conformational change under shear. The decrease of the short periodic energy changes and increase of the long periodic energy changes caused the decrease of required energy for the atom to pass over a certain distance, because the total energy as an integration of the required energy to pass over each potential peak, decreased with decreasing of short periodic energy changes. Accordingly, this was expected to be one of the causes of the shear thinning, though other factors such as anisotropy of pressure and the efficiency of transfer of molecular momentum may also have a role.[15]

It follows from what has been said that branched molecules have somewhat lower shear stress in a confined system and are suitable for magnetic recording disks, though the differences of branched and linear molecules are smaller than SFA experimental results at low slider velocity. The shear behavior of practical-use lubricants is quite different from these simulations and SFA experimental results, because other factors such as chemical decomposition sometimes dominate shear behavior. For example, Fomblin Z is easily decomposed and the slider surface contains more fluorinated metal than in Demnum, Krytox, and Fomblin Y cases. These metal fluorides are expected to lead to lower maximum shear stress and more slips between the slider and the disk surface and the lower frictional surface. Further investigation on the effect of metal fluorides is needed. However, to understand the effects of each factor on the shear behavior, computer simulations are a powerful technique. The combination of precise experiments and computer simulations is important to develop high-performance lubricants.

Acknowledgment. We are grateful for helpful discussions with Prof. S. Granick of Illinois University and Mr. Y. Ito of Hitachi Research Laboratory. We acknowledge the use of the SR2201 parallel computers in the Japan Atomic Energy Research Institute and Dr. H. Kaburaki and Dr. F. Shimizu who advised us about parallelization of the program.

References and Notes

(1) Homola, A. M.; Mate, C. M.; Street, G. B. *MRS Bull.* **1990**, *March*, 45.

(2) Novotony, V. J.; Karis, T. E.; Whitefield, R. J. *Tribol. Trans.* **1997**, *40*, 69.

(3) Rühe, J.; Nobotny, V.; Clarke, T.; Street, G. B. *J. Tribol.* **1996**, *118*, 663.

(4) Gui, J.; Marchon, B. *J. Appl. Phys.* **1995**, *78*, 4206.

(5) Michelle, L. G.; McGuiggan, P. M.; Israelachvili, J. N. *J. Chem. Phys.* **1990**, *93*, 1895.

(6) Granick S.; Demirel, A. L.; Cai, L. L.; Peanasky, J. *Isr. J. Chem.* **1994**, *35*, 75.

(7) Granick, S. *Science* **1991**, *253*, 1374.

(8) Reiter, G.; Demirel, A. L.; Penasky, J.; Cai, L. L.; Granick, S. *J. Chem. Phys.* **1994**, *101*, 2606.
(9) Homola, A. M.; Nguyen, H. V.; Hadziioannou, G. *J. Chem. Phys.* **1991**, *94*, 2346.
(10) Montfort J. P.; Hadziioannou, G. *J. Chem. Phys*. **1988**, *88*, 7187.
(11) Cho, Y.-K.; Granick, S. *Wear* **1996**, *200*, 346.
(12) Dijkstra, M. *J. Phys. Chem.* **1997**, *107*, 3227.
(13) Wang, Y.; Hill, K.; Harris, J. G. *J. Chem. Phys.* **1994**, *100*, 3276.
(14) Davis, P. J.; Evans, D. J.; Morriss, G. P. *J. Chem. Phys.* **1992**, *97*, 616.
(15) Khare, R.; de Pablo, J.; Yethiraj, A. *J. Chem. Phys.* **1997**, *107*, 6956.
(16) Lahtela, M.; Linnolahti, M.; Pakkanen, T. A.; Rowley, R. L. *J. Chem. Phys.* **1998**, *108*, 2626.
(17) Gupta, S. A.; Cochran, H. D.; Cummings, P. T. *J. Chem. Phys.* **1997**, *107*, 10316.
(18) Gupta, S. A.; Cochran, H. D.; Cummings, P. T. *J. Chem. Phys.* **1997**, *107*, 23, 10327.
(19) Gupta, S. A; Cochran, H. D.; Cummings, P. T. *J. Chem. Phys.* **1997**, *107*, 23, 10335.
(20) Stevens, M. J.; Mondello, M.; Grest, G. S.; Cui, S. T.; Cochran, H. D.; Cummings, P. T. *J. Chem. Phys.* **1997**, *106*, 7303.
(21) Thompson, P. A.; Robbins, M. O.; Grest, G. S. *Isr. J. Chem.* **1995**, *35*, 93.
(22) Manufactured by Montefluos (Montedison Group).
(23) Manufactured by DuPont Performance Products.
(24) Manufactured by DAIKIN Industries Ltd.
(25) Pooley C. M.; Tabor, D. *Proc. R. Soc. London A.* **1972**, *329*, 251.
(26) Dauber-Osguthorpe, P.; Roberts, V. A.; Osguthorpe, D. J.; Genest, M.; Hagler, A. T. *Proteins: Struct., Funct., Genet.* **1988**, *4*, 31.
(27) Kittel, H. *Introduction to Solid State Physics*, 6th ed.; Wiley: New York, 1986.
(28) Kong, C. L. *J. Chem. Phys.* **1973**, *59*, 2464.
(29) Theodorou, D. N.; Suter, U. W. *Macromolecules* **1985**, *18*, 1467.
(30) Ferry J. D. *Viscoelastic Properties of Polymers*, 3rd ed.; Wiley: New York, 1980.
(31) Goldstein, H. *Classical Mechanics*; Addison-Wesley: New York, 1969.
(32) Hockney, R. W. *Methods Comput. Phys.* **1976**, *20*, 136.
(33) Berendsen, H. J. C.; Postma, J. P. M.; van Gunsteren, W. F.; DiNola, A.; Haak, J. R. *J. Chem. Phys.* **1984**, *81*, 3684.
(34) Khare, R.; de Pablo, J. J.; Yethiraj, A. *Macromolecules* **1996**, *29*, 7910.
(35) Padilla, P.; Toxvaerd, S. *J. Chem. Phys.* **1994**, *101*, 1490.
(36) Davis, P. J.; Evans, D. J. *J. Chem. Phys.* **1994**, *100*, 541.
(37) Padilla, P.; Toxvaerd, S. *J. Chem. Phys.* **1992**, *97*, 7687.
(38) Allen, M. P.; Tildesley, D. J. *Computer Simulation of Liquids*; Clarendon Press: Oxford, 1996.
(39) Demirel, A. L.; Granick, S. *Phys. Rev. Lett.* **1996**, *77*, 4330.
(40) Bowden, F. P.; Tabor, D. *The Friction and Lubrication of Solids*; Clarendon Press: Oxford, 1950.
(41) Chen, Y. L.; Helm, C. A.; Israelachvili, J. N. *J. Phys. Chem.* **1991**, *95*, 10736.
(42) Yoshizawa, H.; Chen, Y.-L.; Israelachvili, J. N. *Wear* **1993**, *168*, 161.
(43) Thompson, P. A.; Grest, G. S.; Robbins, M. O. *J. Chem. Phys*. **1992**, *68*, 3448.
(44) Koike, A.; Yoneya, M. *J. Phys. Chem.* **1998**, *102*, 3669.
(45) Manias, E.; Hadziioannou, G.; Bitsanis, I.; ten Brinke, G. *Europhys. Lett.* **1993**, *24*, 99.
(46) Thompson, P. A.; Troian, S. M. *Nature* **1997**, *389*, 360.
(47) Koike, A. to be published.
(48) Todd, B. D.; Evans, J. D.; Davis, P. J. *Phys. Rev. E.* **1995**, *52*, 1627.
(49) Paul, W.; Smith, G. D.; Yoon, D. Y.; Farago, B. *Phys. Rev. Lett.* **1988**, *80*, 2346.
(50) Granick, S.; Hu, H.-W.; Carson, G. A. *Langmuir* **1994**, *10*, 3867.
(51) Subbotin, A.; Semenov, A.; Manias, E.; Hadziiannou, G.; ten Brinke, G. *Macromolecules* **1995**, *28*, 3898.